

Papers published in *Hydrology and Earth System Sciences Discussions* are under open-access review for the journal *Hydrology and Earth System Sciences*

Explicitation of an important scale dependence in TOPMODEL using a dimensionless topographic index

A. Ducharne

Laboratoire Sisyphe, CNRS/UPMC, Paris, France

Received: 28 January 2009 – Accepted: 4 February 2009 – Published: 4 March 2009

Correspondence to: A. Ducharne (agnes.ducharne@upmc.fr)

Published by Copernicus Publications on behalf of the European Geosciences Union.

HESSD

6, 1621–1649, 2009

**Explicitation of an
important scale
dependence in
TOPMODEL**

A. Ducharne

Title Page

Abstract

Introduction

Conclusions

References

Tables

Figures

⏪

⏩

◀

▶

Back

Close

Full Screen / Esc

Printer-friendly Version

Interactive Discussion

Abstract

This paper stems from the fact that the topographic index used in TOPMODEL is not dimensionless. In each pixel i in a catchment, it is defined as $x_i = \ln(a_i/S_i)$, where a_i is the specific contributing area per unit contour length and S_i is the topographic slope.

5 In the SI unit system, a_i/S_i is in meters, and the unit of x_i is problematic. Even if all the equations in TOPMODEL are homogeneous, it is confusing to use the logarithm of a non-dimensionless quantity as an index, and we propose a simple solution to this issue in the nowadays widespread cases where the topographic index is computed from a regular raster digital elevation model (DEM). The pixel length C being constant, we can
10 define a dimensionless topographic index $y_i = x_i - \ln C$. Reformulating TOPMODEL's equations to use y_i instead of x_i helps giving the units of all the terms in TOPMODEL's equations. Another advantage is to raise awareness about the scale dependence of these equations via the explicit use of the DEM cell size C outside from the topographic index, in what what can be defined as the transmissivity at saturation per unit contour
15 length T_0/C . We eventually demonstrate, based on various examples from the literature, that both T_0/C and the spatial mean \bar{y} of the proposed dimensionless topographic index are very stable with respect to DEM resolution. This markedly reduces the recalibration necessity when changing DEM resolution, thus offering an efficient rescaling framework.

20 1 Introduction

TOPMODEL was originally introduced by Beven and Kirkby (1979) as a conceptual rainfall-runoff model, describing the contributions of both saturation excess flow and baseflow from the saturated zone to the catchment outflow. Simplifying assumptions, widely known as "TOPMODEL assumptions", allow to relate the spatial distribution of
25 the water table depth to the one of a topographic index (TI), depending in each point of the catchment upon local slope and upslope contributing area. This distribution of the

Explicitation of an important scale dependence in TOPMODEL

A. Ducharne

Title Page

Abstract

Introduction

Conclusions

References

Tables

Figures



Back

Close

Full Screen / Esc

Printer-friendly Version

Interactive Discussion

water table depth controls (i) baseflow owing to the physically-based Darcy's law, and (ii) the extent of the surface saturated area, thus the saturation excess flow, owing to the variable contributing area concept first proposed by Cappus (1960).

This model has been widely used, and not only as a rainfall-runoff model. As high values of the TI reflect a high potential for local saturation, maps of this index have been used to delineate wetlands (e.g. Merot et al., 1995; Curie et al., 2007). Over the last decade, TOPMODEL concepts have also been increasingly used in land surface models to describe the influence of topography on the lateral heterogeneity of runoff, soil moisture, and the coupled surface energy balance, including evapotranspiration (e.g. Famiglietti and Wood, 1994; Peters-Lidars et al., 1997; Stieglitz et al., 1997; Koster et al., 2000; Ducharne et al., 2000; Chen and Kumar, 2001; Decharme and Douville, 2006).

The high popularity of TOPMODEL arises from its simplicity of use, especially since topography has become widely described by digital elevation models (DEMs) from which it is easy to compute the TI. Yet, this apparent simplicity can be misleading, and most users of this model would probably agree on this point. One reason is that "TOPMODEL's assumptions" are together strong but not very intuitive, so that a recurrent anguish when developing new applications of this model is "Don't I violate TOPMODEL's assumptions?" Another reason is related to the fact that the TI is not dimensionless, which is very counter-intuitive and confusing.

This paper elucidates the latter issue (Sect. 2) and proposes a simple solution when a raster DEM is used to compute the TI, as in most present time applications (Sect. 3). The advantages of this simple adaptation of TOPMODEL's framework are discussed in Sect. 4 by comparison with previous attempts to reduce the dependence between the TI distribution, TOPMODEL's parameters and the DEM resolution.

Explicitation of an important scale dependence in TOPMODEL

A. Ducharne

Title Page

Abstract

Introduction

Conclusions

References

Tables

Figures

⏪

⏩

◀

▶

Back

Close

Full Screen / Esc

Printer-friendly Version

Interactive Discussion

2 Classical TOPMODEL's development

The following development of TOPMODEL's equations from its simplifying assumptions is not new and was inspired by many papers, in particular from Beven and Kirkby (1979), Sivapalan et al. (1987), Franchini et al. (1996) and Stieglitz et al. (1997). All

5 notations are defined in Table 1 with their SI unit.

2.1 Scope and assumptions

Let us consider a hydrological catchment of area A . Let us further assume that the topography of this catchment is described by a raster DEM with a pixel length C so that $A=nC^2$, n being the number of pixels in the catchment.

10 To describe the evolution of the table depth over time and space, which is crucial to predict baseflow from the water table and the extent of saturated areas thus saturation excess flow, TOPMODEL relies on four strong assumptions H1 to H4 regarding the behaviour of the modelled catchment:

H1: At each time step, the recharge to the water table $R(t)$ is uniform in the catchment.

15 *H2:* The water table dynamics is approximated by a succession of steady states, so that in each pixel of the catchment and at each time step, the local outflow from the saturated zone equals the recharge from the contributing area. Isolating one time step, over which the uniform recharge rate is R , we can thus write Q_i , the outflow from the saturated zone at any pixel i in the catchment, as

$$20 \quad Q_i = A_i R \quad (1)$$

where A_i is the local contributing area.

H3: In each pixel i , the local hydraulic gradient is approximated by the local topographic slope S_i .

Title Page

Abstract

Introduction

Conclusions

References

Tables

Figures

⏪

⏩

◀

▶

Back

Close

Full Screen / Esc

Printer-friendly Version

Interactive Discussion

Explicitation of an important scale dependence in TOPMODEL

A. Ducharne

Title Page

Abstract

Introduction

Conclusions

References

Tables

Figures

⏪

⏩

◀

▶

Back

Close

Full Screen / Esc

Printer-friendly Version

Interactive Discussion

H4: The saturated hydraulic conductivity K_s is uniform in the catchment but decreases with depth following an exponential law:

$$K_s(z) = K_0 \exp(-\nu z) \quad (2)$$

where z is the depth from the soil surface, $K_0 = K_s(z=0)$ is the saturated hydraulic conductivity at the soil surface, and ν is the saturated hydraulic conductivity decay factor with depth. Both K_0 and ν are uniform in the catchment.

Assumption H4 has been relaxed by Ambroise et al. (1996) and Duan and Miller (1997) regarding the shape of the vertical profile of saturated hydraulic conductivity, and by Beven (1986) regarding the uniformity of K_0 . Assumption H2 has been relaxed by Beven and Freer (2001) using a kinematic wave routing of subsurface flow. Assumption H3, pertaining to the local hydraulic gradient, can also be relaxed, using the concept of reference levels (Quinn et al., 1991). Assumption H1, however, is essential to derive the simple relationship between the local and mean water depths which is at the crux of TOPMODEL (Eq. 13). The only way to relax it is to separate different landscape or hillslope elements within the catchment, as first proposed by Band et al. (1993) and further developed in the finely distributed application of TOPMODEL of Peters-Lidars et al. (1997). For simplicity, we will stick in the following to the original assumptions.

2.2 Towards TOPMODEL's equations

From Darcy's law and assumption H3, the local outflow from the saturated zone at pixel i , across a downstream edge of length L_i , can be written

$$Q_i = L_i T_i S_i. \quad (3)$$

In this expression, T_i is the local transmissivity defined as

$$T_i = \int_{\infty}^{z_i} z K_s(z) dz \quad (4)$$

where z_i is the local depth to the water table. Combining with Eq. (2):

$$T_i = K_0 \int_{\infty}^{z_i} z e^{-vz} dz = \frac{K_0}{v} \exp(-vz_i) = T_0 \exp(-vz_i) \quad (5)$$

where $T_0 = K_0/v$ is the transmissivity of the soil when it is fully saturated ($z_i=0$). Combining Eqs. (1), (3) and (5):

$$Q_i = A_i R = L_i T_0 S_i \exp(-vz_i). \quad (6)$$

Under TOPMODEL's assumptions, this holds everywhere in the catchment, in particular at the outlet which drains the entire catchment. The baseflow from the catchment is thus

$$Q_{\text{out}} = L_{\text{out}} T_0 S_{\text{out}} \exp(-vz_{\text{out}}) \quad (7)$$

where the only unknown is z_{out} , the water table depth at the outlet pixel where the local slope is S_{out} . More generally, the distribution of the local water table depth z_i in the catchment is used to deduce the surface saturated area, which is defined by the pixels where $z_i \leq 0$. Rewriting Eq. (6), z_i can be expressed as follows:

$$z_i = -\frac{1}{v} \ln \left(\frac{A_i R}{L_i T_0 S_i} \right). \quad (8)$$

Introducing $a_i = A_i/L_i$, the specific contributing area per unit contour length, we find the classical TOPMODEL's equation, where the fraction in the natural logarithm is dimensionless:

$$z_i = -\frac{1}{v} \ln \left(\frac{a_i R}{T_0 S_i} \right). \quad (9)$$

Separating, in the natural logarithm, the variables that are uniform in the catchment from the ones that are not, we get

$$z_i = -\frac{1}{v} \left(\ln \frac{R}{T_0} + \ln \frac{a_i}{S_i} \right). \quad (10)$$

The variable term is defined in TOPMODEL as the topographic index (TI)

$$x_i = \ln \frac{a_i}{S_i}. \quad (11)$$

Note that relaxing the assumption that K_0 is uniform leads to another index of lateral heterogeneity, the soil-topographic index $\ln(a_i/T_i S_i)$ (Beven, 1986). In any case, the ratio on which the natural logarithm is applied is not dimensionless.

The mean water table depth \bar{z} is introduced to eliminate the uniform terms

$$\bar{z} = -\frac{1}{v} \left(\ln \left(\frac{R}{T_0} \right) + \bar{x} \right) \quad (12)$$

so that

$$z_i - \bar{z} = -\frac{1}{v} (x_i - \bar{x}) \quad (13)$$

where \bar{x} is the average of x_i over the catchment. This equation, which states that the spatial variations of the water table and the TI are proportional, is probably the most important in the TOPMODEL framework.

It is used to deduce the surface saturated area from the distribution of x_i in the catchment and the mean table depth \bar{z} . Applied to the outlet pixel, with local water table depth and TI z_{out} and x_{out} , it also gives

$$z_{\text{out}} = \bar{z} - \frac{1}{v} (x_{\text{out}} - \bar{x}) \quad (14)$$

which, substituted in Eq. (7), leads to

$$\begin{aligned} Q_{\text{out}} &= L_{\text{out}} T_0 S_{\text{out}} \exp(-v\bar{z} + x_{\text{out}} - \bar{x}) \\ &= L_{\text{out}} T_0 S_{\text{out}} \exp \left(\ln \frac{a_{\text{out}}}{S_{\text{out}}} \right) \exp(-v\bar{z} - \bar{x}) \\ &= a_{\text{out}} L_{\text{out}} T_0 \exp(-v\bar{z} - \bar{x}) \\ Q_{\text{out}} &= A T_0 \exp(-v\bar{z} - \bar{x}). \end{aligned} \quad (15)$$

Using SI units, AT_0 is in $m^4 s^{-1}$, but Q_{out} is in $m^3 s^{-1}$. This results from the fact that $\exp(-\bar{x})$ is in m^{-1} , since x_i is the natural logarithm of a ratio dimensioned in m. Even if Eqs. (10), (12), (13) and (15) are homogeneous, we argue that using the logarithm of a non-dimensionless quantity as an index is confusing. We thus propose a simple modification to prevent from this confusion.

3 Introducing a dimensionless TI to solve the identified scale issue

3.1 Topographic analysis using single-flow direction algorithms

Many methods are available for deriving the slopes S_i and upslope contributing areas A_i from a regular raster DEM. The most simple ones are the single-flow direction (SFD) algorithms, according to which one pixel contributes to only one downslope pixel (e.g. Wolock and Price, 1994). These algorithms rely on the digital terrain analysis (DTA) methods introduced by Jenson and Domingue (1988) and are still very popular (e.g. Wolock and McCabe, 2000; Kumar et al., 2000). In this framework, having defined C as the DEM cell size thus pixel length, we can write that $L_i=C$ and $A_i=n_i C^2$, where n_i is the number of pixels in the contributing area. This leads to

$$x_i = \ln \frac{n_i C}{S_i}. \quad (16)$$

The pixel length C being a constant, we can thus introduce a *dimensionless topographic index*

$$y_i = \ln \frac{n_i}{S_i} \quad (17)$$

which simply relates to x_i

$$x_i = y_i + \ln C. \quad (18)$$

Section 3.2 will show how this expression can be generalized to the more complex cases where multiple-flow direction algorithms (e.g. Quinn et al., 1991) are used to compute a_i , L_i and S_i . In any case, Eq. (10) becomes

$$z_i = -\frac{1}{v} \left(\ln \left(\frac{CR}{T_0} \right) + y_i \right) \quad (19)$$

- 5 where the natural logarithm is applied to two dimensionless terms (CR/T_0 and n_i/S_i). In addition, the DEM resolution is explicit via C .

From there, we can follow the same development with this index as in TOPMODEL with x_i and introduce the mean water table depth \bar{z} to eliminate the uniform terms

$$z_i - \bar{z} = -\frac{1}{v} (y_i - \bar{y}) \quad (20)$$

- 10 where \bar{y} is the average of y_i over the catchment. Applied to the outlet pixel, it gives

$$z_{\text{out}} - \bar{z} = -\frac{1}{v} (y_{\text{out}} - \bar{y}) \quad (21)$$

which, substituted in Eq. (7), leads to

$$\begin{aligned} Q_{\text{out}} &= CT_0 S_{\text{out}} \exp(-v\bar{z} + y_{\text{out}} - \bar{y}) \\ &= CT_0 S_{\text{out}} \exp \left(\ln \frac{n_{\text{out}}}{S_{\text{out}}} \right) \exp(-v\bar{z} - \bar{y}) \\ 15 \quad &= n_{\text{out}} CT_0 \exp(-v\bar{z} - \bar{y}) \\ Q_{\text{out}} &= \frac{AT_0}{C} \exp(-v\bar{z} - \bar{y}) \end{aligned} \quad (22)$$

This expression is of course perfectly equivalent to Eq. (15), except that it relies on a dimensionless TI y , and that the scale dependence of this expression is explicit via the DEM cell size C .

Explicitation of an important scale dependence in TOPMODEL

A. Ducharne

Title Page

Abstract

Introduction

Conclusions

References

Tables

Figures

⏪

⏩

◀

▶

Back

Close

Full Screen / Esc

Printer-friendly Version

Interactive Discussion

3.2 Generalization to multiple-flow direction algorithms

Since their introduction by Quinn et al. (1991), multiple-flow direction (MFD) algorithms have been widely used to compute the TI and regularly improved (e.g. Holmgren, 1994; Quinn et al., 1995; Seibert and McGlynn, 2006). Their basic difference with SFD algorithms is that they distribute the contribution from the upslope contributing area between all the contiguous downslope cells, proportionally to the corresponding slopes.

In this framework, the expression of the specific area drained per unit contour length is not as simple as the one used with SFD methods, what leads to the following general expression of the TI

$$x_i = \ln \left(\frac{A_i}{\sum_{d=1}^{n_d} S_i^d L_i^d} \right) \quad (23)$$

n_d is the total number of downhill directions, S_i^d is the slope between the local pixel i and the neighbouring pixel in the d th downhill direction, and L_i^d is the contour length normal to this direction. Note that this expression also holds for $n_d=1$, which corresponds to the SFD case.

There are many other variations around the general basis provided by the SFD and MFD methods (e.g. Mendicino and Sole, 1997; Tarboton, 1997). Alternatives also exist regarding the way to account for channel or creek pixels (e.g. Saulnier et al., 1997a; Mendicino and Sole, 1997; Sorensen et al., 2006) or the way to determine flow direction and slope in flat areas (e.g. Wolock and McCabe, 1995; Pan et al., 2004; Gascoin et al., 2008). Several papers addressed the comparison of the various DTA methods to derive the TI (Wolock and McCabe, 1995; Mendicino and Sole, 1997; Pan et al., 2004; Sorensen et al., 2006). They all demonstrate the sensitivity of the TI distribution (including the mean TI \bar{x}) to these methods, but their conclusions regarding the relative performances of the different methods are not consistent, apart from a consensus about the superiority of MFD algorithms for divergent hillslopes.

Explicitation of an important scale dependence in TOPMODEL

A. Ducharne

Title Page

Abstract

Introduction

Conclusions

References

Tables

Figures

⏪

⏩

◀

▶

Back

Close

Full Screen / Esc

Printer-friendly Version

Interactive Discussion

In any case, one can always write that $A_i = \alpha_i C^2$ and $L_i^d = \beta_i^d C$, where α_i and β_i^d are dimensionless factors. This leads to the general form of the TI

$$x_i = \ln \left(\frac{\alpha_i C}{\sum_{d=1}^{n_d} S_i^d \beta_i^d} \right) \quad (24)$$

which can be reduced to the dimensionless TI

$$y_i = \ln \left(\frac{\alpha_i}{\sum_{d=1}^{n_d} S_i^d \beta_i^d} \right) = x_i - \ln C \quad (25)$$

owing to the fact that the pixel length C is constant in regular raster DEMs.

4 Articulations with published analyses of scale issues in TOPMODEL

4.1 Interplay between DEM resolution, TI distribution and TOPMODEL's parameters

Many authors studied how the classical TI distribution is impacted by the topographic information content in DEMs, which depends both on the scale of the topographic map the DEM is derived from (Wolock and Price, 1994), and on the DEM resolution, as defined by the pixel length. The latter influence has received considerably more attention and the first-order effect is known as the translation or shift effect, which consists in an increase of mean TI \bar{x} when the DEM resolution decreases, i.e. with coarser cell sizes (e.g. Zhang and Montgomery, 1994; Franchini et al., 1996; Saulnier et al., 1997b; Brasington and Richards, 1998; Higy and Musy, 2000; Valeo and Moin, 2000; Wu et al., 2007).

This shift in \bar{x} leads to larger calibrated transmissivities and saturated hydraulic conductivities when the DEM resolution decreases, as detailed by Franchini et al. (1996). In a catchment, two DEMs with different cell sizes $C_2 > C_1$ correspond to different mean TIs $\bar{x}_2 > \bar{x}_1$. If the calibrated value of TOPMODEL's transmissivity is $T_{0,1}$ for cell size C_1 ,

Title Page

Abstract

Introduction

Conclusions

References

Tables

Figures

⏪

⏩

◀

▶

Back

Close

Full Screen / Esc

Printer-friendly Version

Interactive Discussion

Explicitation of an important scale dependence in TOPMODEL

A. Ducharne

Title Page

Abstract

Introduction

Conclusions

References

Tables

Figures

⏪

⏩

◀

▶

Back

Close

Full Screen / Esc

Printer-friendly Version

Interactive Discussion

the shift effect can be compensated by a simple recalibration of this transmissivity to $T_{0,2}$, such as to maintain the relationship between TOPMODEL's baseflow Q^* and the mean water table depth \bar{z}^* . Following Franchini et al. (1996), we assume constant ν for simplicity, so that

$$5 \quad Q^* = AT_{0,1} \exp(-\nu\bar{z}^* - \bar{x}_1) = AT_{0,2} \exp(-\nu\bar{z}^* - \bar{x}_2). \quad (26)$$

This leads to the following relationship between the transmissivities and mean TIs:

$$T_{0,2} = T_{0,1} \exp(\bar{x}_2 - \bar{x}_1). \quad (27)$$

The dimensionless index y is very much inspired by this pioneering work of Franchini et al. (1996), and it allows including the DEM cell size in the above relationship and in the associated change in mean classical TI:

$$10 \quad T_{0,2} = T_{0,1} \frac{C_2}{C_1} \exp(\bar{y}_2 - \bar{y}_1) \quad (28)$$

$$\bar{x}_2 = \bar{x}_1 + \ln \frac{C_2}{C_1} + (\bar{y}_2 - \bar{y}_1). \quad (29)$$

This set of equations clearly highlights that the changes in T_0 and mean classical TI \bar{x} when the DEM resolution varies arises from two different causes, as summarized in Table 2:

- a numerical effect, because the DEM cell size C enters into the expression of a_j . When using the dimensionless TI, the influence of this effect on T_0 is explicitated by the scaling factor C_2/C_1 in Eq. (28);
- a terrain effect, owing to the influence of DEM resolution on both the local slopes S_j and the shape of the hydrographic network, thus a_j . Following Wolock and McCabe (2000), this terrain effect can itself be separated in two components: a discretization effect, which arises from dividing the terrain in different numbers of grid cells; and a smoothing effect, related to decreased variability of the local

Explicitation of an important scale dependence in TOPMODEL

A. Ducharne

Title Page	
Abstract	Introduction
Conclusions	References
Tables	Figures
⏪	⏩
◀	▶
Back	Close
Full Screen / Esc	
Printer-friendly Version	
Interactive Discussion	

slopes when using coarser resolution DEMs, what filters the terrain roughness (Valeo and Moin, 2000). The overall terrain effect has consequences on both the shape of the TI distribution and on its mean. The effect on the mean contributes to the shift effect, and its consequence on T_0 is isolated in the term $\exp(\bar{y}_2 - \bar{y}_1)$ of Eq. (28).

Yet, K_0 , which controls T_0 , may influence the recharge of the water table, and \bar{x} controls the extent of the saturated zone, thus the partitioning between surface runoff and water table recharge. As a result, Eq. (26) and the related rescaling of T_0 to compensate the shift effect are strictly valid for one timestep only. This rescaling may thus not be enough to achieve as realistic flows as the ones obtained by the real calibration of T_0 using the TI distribution derived with cell size C_2 , as reported by Saulnier et al. (1997b) in the Maurets catchment (described in Table 3). This limitation of the rescaling of T_0 aiming at compensating the shift effect is attributed to the fact that, in this catchment, the DEM resolution not only influences the mean TI but also the shape of the TI distribution. The authors eventually propose an efficient scaling factor for K_0 , deduced from the differences in TI cumulative distributions when the DEM resolution changes.

4.2 Advantages of the dimensionless topographic index in real-world case studies

In the extensive literature devoted to the influence of DEM resolution onto the TI distribution and the performances of TOPMODEL, we could find six papers allowing us to calculate the mean of the dimensionless index \bar{y} for different DEM cell sizes C . The six corresponding case studies are summarized in Table 3. Note that the Maurets catchment (Saulnier et al., 1997b) is a subcatchment of the experimental research catchment of the Réal Collobrier (Franchini et al., 1996), and that mean TIs from two different DTAs, namely the SFD and MFD algorithms, are available in the sub-catchment W3 of the Sleepers River (Wolock and McCabe, 1995).

The 7 resulting cases confirm that, once chosen the DTA method to compute the TI, the mean of the classical index \bar{x} increases with DEM cell size C (Table 4), a rule



that we could not find invalidated in the literature. Based on the values gathered in Table 4, the mean classical TI \bar{x} exhibits variation rates between 0.005 and 0.02, the related unit being $\ln(m) m^{-1}$. In contrast, positive variation rates are not systematic for the mean dimensionless TI \bar{y} .

More importantly, these variation rates show that the mean dimensionless TI \bar{y} varies much less with DEM resolution than does the mean classical TI \bar{x} , in all the 7 studied cases. This result was expected from the definition of the dimensionless TI, and is further illustrated in Fig. 1, where the trajectories followed by \bar{y} span smaller ranges than the ones followed by \bar{x} under the same DEM resolution changes. Of course, the units are different and there is no point comparing \bar{x} and \bar{y} for the same DEM resolution. Their changes when DEM resolution varies, however, are important as they motivate the rescaling of transmissivity (Sect. 4.1).

Figure 1 also shows that the variations of \bar{x} due to DEM resolution exceed the ones related to the DTA methods and the location of the catchments, which controls their specific topographical features. As a result, one cannot isolate the different locations from the variability induced on \bar{x} by the DEM resolution. In contrast, one can separate the projections of the different trajectories on the vertical axis representing \bar{y} , what shows that the mean dimensionless TI can efficiently discriminate the different locations, regardless of DEM resolution.

This is illustrated by the correlations between the altitude range and the mean TIs of the 6 selected catchments (Fig. 2). Fixing the DEM resolution, this correlation is highly negative with the mean of both TIs, what probably results from the fact that local slopes are higher in catchments with an important altitude range. The comparison of the two panels in Fig. 2, however, shows that if care is not taken to use the same DEM resolution when comparing mean TIs between catchments, the relationship between mean TI and altitude range is completely hidden with \bar{x} whereas it is detectable with \bar{y} .

The above results are linked to the fact that, at least in the selected catchments, the shift effect on \bar{x} is largely dominated by the numerical effect, which is absent by construction when using the dimensionless TI. The remaining DEM resolution effect

Explicitation of an important scale dependence in TOPMODEL

A. Ducharne

Title Page

Abstract

Introduction

Conclusions

References

Tables

Figures

⏪

⏩

◀

▶

Back

Close

Full Screen / Esc

Printer-friendly Version

Interactive Discussion

is then the terrain effect, which is small enough in the 6 studied catchments to be neglected at first order. If confirmed, this would imply that the mean dimensionless TI \bar{y} is almost independent of DEM resolution.

The consequence, if the terrain effect quantified by $\exp(\bar{y}_2 - \bar{y}_1)$ can be neglected when the DEM resolution changes, is that Eq. (28) can be approximated to

$$\frac{T_{0,2}}{C_2} \simeq \frac{T_{0,1}}{C_1}. \quad (30)$$

This result is confirmed by Table 5, which shows that the calibrated values of T_0/C or K_0/C exhibit considerably less variations with C than do the calibrated values of T_0 or K_0 . A further consequence is thus to reduce the need to recalibrate TOPMODEL when using the dimensionless TI, as T_0/C becomes an explicit parameter (Eq. 22), which can be defined as the transmissivity at saturation per unit contour length (in m s^{-1}).

4.3 Articulations with alternative rescaling techniques

The scaling factors proposed by Franchini et al. (1996) and Saulnier et al. (1997b) can be used to guide and facilitate the required recalibration of TOPMODEL' transmissivity when changing the DEM resolution. Other scaling techniques were later proposed to rather rescale the classical TI distribution, such as to limit the need to recalibrate the transmissivity.

From a regression analysis using a sample of 50 quadrangles of $1^\circ \times 1^\circ$ ($\simeq 7000 \text{ km}^2$) in the conterminous USA, Wolock and McCabe (2000) proposed a linear relationship to rescale the mean TIs obtained from a 1000-m resolution DEM (\bar{x}_{1000}) to values that would correspond to a 100-m resolution DEM (\bar{x}_{100}):

$$\bar{x}_{100} = -1.957 + 0.961\bar{x}_{1000}. \quad (31)$$

This linear regression is characterized by a high determination coefficient $R^2=0.93$, and has been widely used (e.g. Kumar et al., 2000; Ducharne et al., 2000; Niu et al.,

Explicitation of an important scale dependence in TOPMODEL

A. Ducharne

Title Page

Abstract

Introduction

Conclusions

References

Tables

Figures

⏪

⏩

◀

▶

Back

Close

Full Screen / Esc

Printer-friendly Version

Interactive Discussion



2005; Decharme and Douville, 2006). It can easily be extended to the dimensionless TI

$$\bar{y}_{100} = 0.525 + 0.961\bar{y}_{1000} \quad (32)$$

and the smaller y -intercept in Eq. (32) than in Eq. (31) confirms that \bar{y} depends less on DEM resolution than \bar{x} , owing to the elimination of the numerical effect of DEM resolution.

Mendicino and Sole (1997) analysed the simulations of 11 flood events by TOPMODEL in the Turbolo Creek (29 km², in Italy), using a 30-m resolution DEM, aggregated to coarser resolutions (90-m, 150-m and 270-m). They proposed a linear relationship between the mean TI and a spatial variability measure (SVM), which describes the topographic information content of the DEM following Shannon and Weaver (1949), and depends on DEM resolution by a simple function of the number of grid cells.

This approach was further explored by Ibbitt and Woods (2004) in a 50-km² catchment in New Zealand, with similar results. These authors also provided evidence of a linear relationship between $\bar{x}(C)$ and $\log_{10}(C)$, which is perfectly consistent with the facts that $\bar{y} = \bar{x} - \ln C$ (from Eq. 18) and that \bar{y} undergoes negligible variations with C (Sect. 4.2). This relationship is thus verified in the catchments of Table 4, the correlation coefficient between $\bar{x}(C)$ and $\log_{10}(C)$ exceeding 0.99 in all seven cases.

Combining the two linear relationships between \bar{x} , SVM and C , Ibbitt and Woods (2004) could define the DEM resolution that maximized the topographic information content: $SVM(C)=1 \Rightarrow C=2$ cm, which corresponds to the scale of saturated conductivity measurements. Rescaling the TI distribution to such resolution renders possible to use in situ measurements of the saturated hydraulic conductivity K_0 , which is otherwise forbidden by the interdependence between the DEM resolution, the mean classical TI and K_0 .

Another method, aiming at rescaling the entire distribution of the classical TI instead of its mean, was proposed by Pradhan et al. (2006) in the Kamishiiba catchment (Table 3), where TI distributions were derived at 5 different DEM resolutions using a SFD

Explicitation of an important scale dependence in TOPMODEL

A. Ducharne

Title Page

Abstract

Introduction

Conclusions

References

Tables

Figures

⏪

⏩

◀

▶

Back

Close

Full Screen / Esc

Printer-friendly Version

Interactive Discussion

algorithm. The TI $x_{i,2}$ scaled at the target cell size C_2 from a coarser DEM with a cell size C_1 is expressed as

$$x_{i,2} = \ln \frac{a_{i,1}}{S_{i,2}} - \ln C_1 + \ln C_2 - \ln I_f. \quad (33)$$

In this equation, I_f describes the terrain discretization effect (see Sect. 4.1) on the upslope contributing area. It depends on the two DEM cell sizes C_1 and C_2 , and on the numbers of pixels at the coarser resolution in both the upslope contributing area and in the entire catchment. The authors also propose an interesting way to deduce the local slopes $S_{i,2}$ at the target resolution from the coarser DEM and a fractal method to introduce steepest slopes. Rearranging Eq. (33), by keeping in mind that I_f varies within the catchment, leads to

$$x_{i,2} = \ln \left(\frac{n_{i,1}}{I_f S_{i,2}} \right) + \ln C_2. \quad (34)$$

Table 2 separated three different DEM effects onto the classical TI distribution and quantified how the effects on mean TI propagated on rescaled saturated hydraulic conductivity. These three effects also appear in the above equation, where one can isolate the numerical effect in $\ln C_2$, whereas the discretization effect originates from I_f and the smoothing effect from the rescaled slopes $S_{i,2}$. Note also that Eq. (34) is very close to Eq. (18), if one considers that the first term in the right-hand side can be seen as a scaled dimensionless TI, which is by construction free from the numerical effect.

5 Conclusions

We argue that replacing x_i , the classical TI of TOPMODEL, by the dimensionless TI $y_i = x_i - \ln C$, makes TOPMODEL's main equations, then replaced by Eqs. (20) and (22), more accessible and less confusing. In particular, this helps giving the units of all the variables (see Table 1), what is lacking in most papers about TOPMODEL, including

Explicitation of an important scale dependence in TOPMODEL

A. Ducharne

Title Page

Abstract

Introduction

Conclusions

References

Tables

Figures

⏪

⏩

◀

▶

Back

Close

Full Screen / Esc

Printer-friendly Version

Interactive Discussion



the most cited ones (e.g. Beven and Kirkby, 1979; Sivapalan et al., 1987), probably by reluctance to use the logarithm of a length as a unit.

Another advantage of using the dimensionless TI in TOPMODEL's equations is that their dependence on DEM cell size C becomes explicit, whereas it is hidden in the TI when using the classical formulation. This is a good way to raise awareness of hydrologists about the scale and resolution issues in TOPMODEL's framework. The dependence on C does not vanish in this process, but it is shifted from the classical TI, where it is related to the upslope contributing area per unit contour length, towards the equation of baseflow (Eq. 22), via T_0/C which can be defined as the transmissivity at saturation per unit contour length.

We further demonstrated that the distribution of the dimensionless TI undergoes a lesser sensitivity to DEM resolution than the one of the classical TI, because it is free from the numerical effect, introduced in Sect. 4.1 as the direct effect of using the cell size in the definition of the classical TI.

We also provided evidence, based on 6 real-world case studies from the literature, that the DEM resolution influence on the mean classical TI \bar{x} was largely dominated by this numerical effect, so that the mean dimensionless TI \bar{y} was almost independent from DEM resolution (Sect. 4.2). If confirmed, this result would have important consequences, as:

- the mean dimensionless TI could be used as an efficient indicator to compare the topographic features of different catchments, regardless of DEM resolution;
- the transmissivity at saturation per unit contour length T_0/C would also be independent from DEM resolution. It would thus not need to be recalibrated if the DEM resolution changed, whereas it is the case when using the classical TI in the classical TOPMODEL's framework, because of the interplay between DEM resolution, mean classical TI and transmissivity.

Finally, and even if the stability of mean dimensionless TI with respect to DEM resolution could not be generalized, this new index can be seen as an interesting bridge be-

Explicitation of an important scale dependence in TOPMODEL

A. Ducharne

Title Page

Abstract

Introduction

Conclusions

References

Tables

Figures



Back

Close

Full Screen / Esc

Printer-friendly Version

Interactive Discussion



tween the two rescaling strategies developed within the classical TOPMODEL's framework to reduce recalibration when DEM resolution changes, namely the rescaling of transmissivity and the rescaling of the TI distribution.

Acknowledgements. This paper benefited from fruitful discussions with Simon Gascoin and Pierre Ribstein, from the Laboratoire Sisyphe. The author also wishes to thank Jan Seibert for his valuable comments as editor of a previous version of this manuscript.

References

- Ambroise, B., Beven, K. J., and Freer, J.: Toward a generalization of the TOPMODEL concepts: topographic indices of hydrological similarity, *Water Resour. Res.*, 32, 2135–2145, 1996. 1625
- Band, L. E., Patterson, P., Nemani, R., and Running, S. W.: Forest ecosystem processes at the watershed scale: incorporating hillslope hydrology, *Agr. Forest Meteorol.*, 63, 93–126, 1993. 1625
- Beven, K.: Hillslope runoff processes and flood frequency characteristics, in: *Hillslope Processes*, edited by: Abrahams, S. D., 187–202, Allen and Unwin, Boston, 1986. 1625, 1627
- Beven, K. and Freer, J.: A dynamic TOPMODEL, *Hydrol. Process.*, 15, 1993–2011, 2001. 1625
- Beven, K. and Kirkby, M. J.: A physically based variable contributing area model of basin hydrology, *Hydrol. Sci. B.*, 24, 43–69, 1979. 1622, 1624, 1638
- Brasington, J. and Richards, K.: Interactions between model predictions, parameters and DTM scales for TOPMODEL, *Comput. Geosci.*, 24, 299–314, doi:10.1016/S0098-3004(97)00081-2, 1998. 1631, 1645, 1646, 1647
- Brasington, J. and Richards, K.: Turbidity and suspended sediment dynamics in small catchments in the Nepal Middle Hills, *Hydrol. Process.*, 14, 2559–2574, 2000. 1645
- Cappus: Etude des lois d'écoulement – application au calcul et à la prévision des débits, *Bassin expérimental d'Alrance, La Houille Blanche*, 60, 493–520, 1960. 1623
- Chen, J. and Kumar, P.: Topographic influence on the seasonal and interannual variation of water and energy balance of basins in North America, *J. Climate*, 14, 1989–2014, 2001. 1623
- Curie, F., Gaillard, S., Ducharne, A., and Bendjoudi, H.: Geomorphological methods to char-

Explicitation of an important scale dependence in TOPMODEL

A. Ducharne

Title Page

Abstract

Introduction

Conclusions

References

Tables

Figures

⏪

⏩

◀

▶

Back

Close

Full Screen / Esc

Printer-friendly Version

Interactive Discussion



- acterize wetlands at the scale of the Seine watershed, *Sci. Total Environ.*, 375, 59–68, doi:10.1016/j.scitotenv.2006.12.013, 2007. 1623
- Decharme, B. and Douville, H.: Introduction of a sub-grid hydrology in the ISBA land surface model, *Clim. Dynam.*, 26, 65–78, doi:10.1007/s00382-005-0059-7, 2006. 1623, 1636
- 5 Duan, J. and Miller, N. L.: A generalized power function for the subsurface transmissivity profile in TOPMODEL, *Water Resour. Res.*, 33, 2559–2562, 1997. 1625
- Ducharne, A., Koster, R. D., Suarez, M., Stieglitz, M., and Kumar, P.: A catchment-based approach to modeling land surface processes in a GCM – Part 2: Parameter estimation and model demonstration, *J. Geophys. Res.*, 105, 24 823–24 838, 2000. 1623, 1635
- 10 Famiglietti, J. S. and Wood, E. F.: Multiscale modeling of spatially variable water and energy balance processes, *Water Resour. Res.*, 30, 3061–3078, 1994. 1623
- Franchini, M., Wendling, J., Obled, C., and Todini, E.: Physical interpretation and sensitivity analysis of the TOPMODEL, *J. Hydrol.*, 175, 293–338, 1996. 1624, 1631, 1632, 1633, 1635, 1645, 1646, 1647
- 15 Gascoïn, S., Ducharne, A., Ribstein, P., Carli, M., and Habets, F.: Adaptation of a catchment-based land surface model to the hydrogeological setting of the Somme River basin (France), *J. Hydrol.*, in press, doi:10.1016/j.jhydrol.2009.01.039, 2009. 1630
- Higy, C. and Musy, A.: Digital terrain analysis of the Haute-Mentue catchment an scale effect for hydrological modelling with TOPMODEL, *Hydrol. Earth Syst. Sci.*, 4, 225–237, 2000, http://www.hydrol-earth-syst-sci.net/4/225/2000/. 1631, 1645, 1646, 1647
- 20 Holmgren, P.: Multiple flow direction algorithms for runoff modelling in grid based elevation models: An empirical evaluation, *Hydrol. Process.*, 8, 327–334, 1994. 1630
- Ibbitt, R. and Woods, R.: Re-scaling the topographic index to improve the representation of physical processes in catchment models, *J. Hydrol.*, 293, 205–218, doi:10.1016/j.jhydrol.2004.01.016, 2004. 1636
- 25 Iorgulescu, I. and Jordan, J.-P.: Validation of TOPMODEL on a small Swiss catchment, *J. Hydrol.*, 159, 255–273, 1994. 1645
- Jenson, S. K. and Domingue, J. O.: Extracting topographic structure from digital elevation data for geographic information system analysis, *Photogramm. Eng. Rem. S.*, 54, 1593–1600, 1988. 1628
- 30 Koster, R. D., Suarez, M., Ducharne, A., Stieglitz, M., and Kumar, P.: A catchment-based approach to modeling land surface processes in a GCM – Part 1: Model structure, *J. Geophys. Res.*, 105, 24809–24822, 2000. 1623

Explicitation of an important scale dependence in TOPMODELA. Ducharne

[Title Page](#)[Abstract](#)[Introduction](#)[Conclusions](#)[References](#)[Tables](#)[Figures](#)[⏪](#)[⏩](#)[◀](#)[▶](#)[Back](#)[Close](#)[Full Screen / Esc](#)[Printer-friendly Version](#)[Interactive Discussion](#)

- Kumar, P., Verdin, K. L., and Greenlee, S. K.: Basin level statistical properties of topographic index for North America, *Adv. Water Resour.*, 23, 571–578, 2000. 1628, 1635
- Lee, G., Tachikawa, Y., and Takara, K.: Analysis of hydrologic model parameter characteristics using automatic global optimization method, *Ann. Disaster Prevention Res. Inst.*, 67–80, 2006. 1645
- Mendicino, G. and Sole, A.: The information content theory for the estimation of the topographic index distribution used in TOPMODEL, *Hydrol. Process.*, 11, 1099–1114, 1997. 1630, 1636
- Merot, P., Ezzahar, B., and Walter, C., and Arousseau, P.: Mapping waterlogging of soils using digital terrain models, *Hydrol. Process.*, 9, 27–34, 1995. 1623
- Niu, G.-Y., Yang, Z.-L., Dickinson, R. E., and Gulden, L. E.: A simple TOPMODEL-based runoff parameterization (SIMTOP) for use in global climate models, *J. Geophys. Res.*, 110, D21106, doi:10.1029/2005JD006111, 2005. 1635
- Obled, C., Wendling, J., and Beven, K.: The sensitivity of hydrological models to spatial rainfall patterns: an evaluation using observed data, *J. Hydrol.*, 159, 305–333, 1994. 1645
- Pan, F., Peters-Lidard, C. D., Sale, M. J., and King, A. W.: Comparison of geographical information systems-based algorithms for computing the TOPMODEL topographic index, *Water Resour. Res.*, 40, W06303, doi:10.1029/2004WR003069, 2004. 1630
- Peters-Lidars, C. D., Zion, M. S., and Wood, E. F.: A soil-vegetation-atmosphere transfer scheme for modelling spatially variable water and energy balance processes, *J. Geophys. Res.*, 102, 4303–4324, 1997. 1623, 1625
- Pradhan, N. R., Tachikawa, Y., and Takara, K.: A downscaling method of topographic index distribution for matching the scales of model application and parameter identification, *Hydrol. Process.*, 20, 1385–1405, 2006. 1636, 1645, 1646, 1647
- Quinn, P., Beven, K., Chevallier, P., and Planchon, O.: The prediction of hillslope flow paths for distributed hydrological modelling using digital terrain models, *Hydrol. Process.*, 5, 59–79, 1991. 1625, 1629, 1630
- Quinn, P., Beven, K., and Lamb, R.: The $\ln(a/\tan B)$ index: how to calculate it and how to use it within the TOPMODEL framework, *Hydrol. Process.*, 9, 161–182, 1995. 1630
- Saulnier, G.-M., Beven, K., and Obled, C.: Digital elevation analysis for distributed hydrological modelling: reducing scale dependence in effective hydraulic conductivity values, *Water Resour. Res.*, 33, 2097–2101, 1997a. 1630
- Saulnier, G.-M., Obled, C., and Beven, K.: Analytical compensation between DTM grid resolution and effective values of saturated hydraulic conductivity within the TOPMODEL frame-

Explicitation of an important scale dependence in TOPMODEL

A. Ducharne

Title Page

Abstract

Introduction

Conclusions

References

Tables

Figures

⏪

⏩

◀

▶

Back

Close

Full Screen / Esc

Printer-friendly Version

Interactive Discussion

Explicitation of an important scale dependence in TOPMODEL

A. Ducharne

Title Page

Abstract

Introduction

Conclusions

References

Tables

Figures

⏪

⏩

◀

▶

Back

Close

Full Screen / Esc

Printer-friendly Version

Interactive Discussion



- work, Hydrol. Process., 11, 1331–1346, 1997b. 1631, 1633, 1635, 1645, 1646, 1647
- Seibert, J. and McGlynn, B. L.: A new triangular multiple flow direction algorithm for computing upslope areas from gridded digital elevation models, Water Resour. Res., 43, W04501, doi:10.1029/2006WR005128, 2006. 1630
- 5 Shannon, C. E. and Weaver, W.: The Mathematical Theory of Communication, University of Illinois Press, Urbana, IL, 117 pp., 1949. 1636
- Sivapalan, M., Beven, K., and Wood, E. F.: On hydrologic similarity: 2. A scaled model of storm runoff production, Water Resour. Res., 23, 2266–2278, 1987. 1624, 1638
- Sørensen, R., Zinko, U., and Seibert, J.: On the calculation of the topographic wetness index: evaluation of different methods based on field observations, Hydrol. Earth Syst. Sci., 10, 101–112, 2006, http://www.hydrol-earth-syst-sci.net/10/101/2006/. 1630
- 10 Stieglitz, M., Rind, M., Famiglietti, J., and Rosenzweig, C.: An efficient approach to modeling the topographic control of surface hydrology for regional and global modeling, J. Climate, 10, 118–137, 1997. 1623, 1624
- 15 Tarboton, D. G.: A new method for the determination of flow directions and upslope areas in grid digital elevation models, Water Resour. Res., 33, 309–319, 1997. 1630
- Valeo, C. and Moin, S. M. A.: Grid-resolution effects on a model for integrating urban and rural areas, Hydrol. Process., 14, 2505–2525, 2000. 1631, 1633
- 20 Wolock, D. and McCabe, G.: Differences in topographic characteristics computed from 100- and 1000-meter resolution digital elevation model data, Hydrol. Process., 14, 987–1002, 2000. 1628, 1632, 1635
- Wolock, D. M. and McCabe, G. J.: Comparison of single and multiple flow direction algorithms for computing topographic parameters in TOPMODEL, Water Resour. Res., 31, 1315–1324, 1995. 1630, 1633, 1645, 1646, 1647
- 25 Wolock, D. M. and Price, C. V.: Effects of digital elevation model map scale and data resolution on a topography-based watershed model, Water Resour. Res., 30, 3041–3052, 1994. 1628, 1631
- Wu, S., Li, J., and Huang, G. H.: Modeling the effects of elevation data resolution on the performance of topography-based watershed runoff simulation, Environ. Modell. Softw., 22, 1250–1260, doi:10.1016/j.envsoft.2006.08.001, 2007. 1631
- 30 Zhang, W. and Montgomery, D. R.: Digital elevation model grid size, landscape representation, and hydrologic simulations, Water Resour. Res., 30, 1019–1028, 1994. 1631

Table 1. Notations and units (pertaining to Sects. 2 and 3.1).

Variable	SI unit	Description
a_i	m	Specific contributing area per unit contour length
a_{out}	m	Specific contributing area per unit contour length at the outlet ($a_{\text{out}}=A/L_{\text{out}}$)
A	m ²	Catchment area
C	m	DEM resolution (pixel length)
h_i	m	Local altitude at pixel i
K_s	m s ⁻¹	Saturated hydraulic conductivity
K_0	m s ⁻¹	Saturated hydraulic conductivity at the surface
L_i	m	Downhill contour length at pixel i
L_{out}	m	Downhill contour length at the outlet pixel
n	–	Number of pixels in the catchment
n_i	–	Local number of upslope pixels at pixel i
n_{out}	–	Local number of upslope pixels at the outlet ($n=n_{\text{out}}$)
p_i	m	Local piezometric head at pixel i
Q_i	m ³ s ⁻¹	Outflow from the saturated area at pixel i
Q_{out}	m ³ s ⁻¹	Outflow from the saturated area at the outlet, or baseflow from the catchment
R	m s ⁻¹	Uniform recharge rate in the catchment
S_j	–	Local topographic slope at pixel i
S_{out}	–	Local topographic slope at the outlet
T_i	m ² s ⁻¹	Local transmissivity of the saturated zone at pixel i
T_0	m ² s ⁻¹	Local transmissivity of at saturation, assumed uniform in the catchment (H4)
x_i	ln(m)	Classical topographic index at pixel i
\bar{x}	ln(m)	Catchment average of the classical topographic index
y_i	–	Dimensionless topographic index at pixel i
y_{out}	–	Dimensionless topographic index at the outlet
\bar{y}	–	Catchment average of the dimensionless topographic index
z_i	m	Local water table depth at pixel i
z_{out}	m	Local water table depth at the outlet
\bar{z}	m	Catchment average of the water table depth
ν	m ⁻¹	Saturated hydraulic conductivity decay factor with depth

Title Page

Abstract

Introduction

Conclusions

References

Tables

Figures

◀

▶

◀

▶

Back

Close

Full Screen / Esc

Printer-friendly Version

Interactive Discussion

Explicitation of an important scale dependence in TOPMODEL

A. Ducharne

Table 2. DEM resolution effects in TOPMODEL’s framework: separation of the DEM resolution effects on the distribution of the classical TI x , and quantification of the related changes in mean TI vs. saturated hydraulic conductivity and transmissivity. Following Eqs. (28) and (29), the grid cell size is assumed to vary from C_1 to C_2 , with subsequent changes in the mean dimensionless TI from \bar{y}_1 to \bar{y}_2 .

DEM resolution effects	Influence on TI distribution		Quantified effect on	
	Shape	\bar{x} (Shift effect)	\bar{x}	K_0 and T_0
Numerical		×	$\ln(C_2/C_1)$	C_2/C_1
Discretization	×	×		
Terrain			$\bar{y}_2 - \bar{y}_1$	$\exp(\bar{y}_2 - \bar{y}_1)$
Smoothing	×	×		

Title Page

Abstract Introduction

Conclusions References

Tables Figures

⏪ ⏩

◀ ▶

Back Close

Full Screen / Esc

Printer-friendly Version

Interactive Discussion



Explicitation of an important scale dependence in TOPMODEL

A. Ducharne

Table 3. Main features of the selected case studies. DTA means Digital Terrain Analysis, and SFD and MFD stand for single and multiple-flow direction algorithms for the TI computation.

Catchment	Reference	Location	Area (km ²)	Altitude range (m)	Map scale	Min(C)	Max(C)	DTA method
Sleepers-W3	Wolock and McCabe (1995)	Vermont, USA	8.4	621	1:24 000	30-m	90-m	SFD and MFD
Réal Collobrier	Franchini et al. (1996)	France	71	700 ^a	?	60-m	480-m	MFD
Maurets	Saulnier et al. (1997b)	France	8.4	561	1:25 000	20-m	120-m	MFD
Bore Khola	Brasington and Richards (1998)	Nepal	4.5	1290 ^b	1:5000	20-m	500-m	MFD
Haute-Mentue	Higy and Musy (2000)	Switzerland	12	236 ^c	1:25 000	25-m	150-m	MFD ^c
Kamishiiba	Pradhan et al. (2006)	Japan	210	≈1400 ^d	?	50-m	1000-m	SFD

^a from Obled et al. (1994)

^b from Brasington and Richards (2000)

^c from Iorgulescu and Jordan (1994)

^d from Lee et al. (2006)

Title Page

Abstract

Introduction

Conclusions

References

Tables

Figures

⏪

⏩

◀

▶

Back

Close

Full Screen / Esc

Printer-friendly Version

Interactive Discussion

Explicitation of an important scale dependence in TOPMODEL

A. Ducharne

Table 4. Mean values of the classical and dimensionless TIs \bar{x} and \bar{y} for 6 different catchments and different DEM resolutions. The reported values come from the literature (see Table 3). The last column gives the mean variation rate of \bar{x} and \bar{y} with DEM resolution.

Sleepers-W3 (Wolock and McCabe, 1995)												
$\Delta/\Delta C$ Resolution (m)	30	60	90								$\Delta/\Delta C$	
\bar{x}	6.56	7.31	7.73	(SFD)							0.020	
\bar{y}	3.16	3.22	3.23	(SFD)							0.001	
\bar{x}	7.30	8.02	8.41	(MFD)							0.019	
\bar{y}	3.90	3.93	3.91	(MFD)							0.000	
Réal Collobrier (Franchini et al., 1996)												
Resolution (m)	60	120	180	240	360	480					$\Delta/\Delta C$	
\bar{x}	7.31	8.01	8.60	9.01	9.77	10.18					0.006	
\bar{y}	3.22	3.22	3.41	3.53	3.88	4.00					0.002	
Maurets (Saulnier et al., 1997b)												
Resolution (m)	20	40	60	80	100	120					$\Delta/\Delta C$	
\bar{x}	6.18	6.60	6.93	7.20	7.42	7.70					0.015	
\bar{y}	3.18	2.90	2.84	2.82	2.82	2.91					-0.002	
Bore Khola (Brasington and Richards, 1998)												
Resolution (m)	20	40	60	80	100	200	300	400	500		$\Delta/\Delta C$	
\bar{x}	6.12	6.67	6.78	7.03	7.26	7.88	8.40	8.70	8.87		0.006	
\bar{y}	3.12	2.98	2.69	2.65	2.65	2.58	2.70	2.71	2.66		-0.001	
Haute-Mentue (Higy and Musy, 2000)												
Resolution (m)	25	30	50	60	75	80	100	110	125	130	150	$\Delta/\Delta C$
\bar{x}	7.98	8.16	8.47	8.67	8.68	8.91	9.03	9.15	9.25	9.45	9.45	0.011
\bar{y}	4.76	4.76	4.56	4.58	4.36	4.53	4.42	4.45	4.42	4.58	4.44	-0.000
Kamishiiba (Pradhan et al., 2006)												
Resolution (m)	50	150	450	600	1000						$\Delta/\Delta C$	
\bar{x}	6.08	7.42	9.22	9.62	10.35						0.005	
\bar{y}	2.17	2.41	3.11	3.22	3.44						0.000	

Title Page

Abstract Introduction

Conclusions References

Tables Figures

⏪ ⏩

◀ ▶

Back Close

Full Screen / Esc

Printer-friendly Version

Interactive Discussion



Table 5. Values of the calibrated transmissivity parameters (T_0 or K_0) and their ratio to the pixel length C for 6 different catchments and different DEM resolutions. The reported values come from the literature (see Table 3). The last column gives the mean variation rate of the parameters with DEM resolution.

Sleepers-W3 (Wolock and McCabe, 1995)												
Resolution (m)	30	60	90								$\Delta/\Delta C$	
T_0 ($m^2 s^{-1}$)	84.34	193.09	295.64	(SFD)							3.52	
T_0/C ($m s^{-1}$)	2.81	3.22	3.28	(SFD)							0.008	
T_0 ($m^2 s^{-1}$)	182.18	328.11	441	(MFD)							4.31	
T_0/C ($m s^{-1}$)	6.07	5.47	4.9	(MFD)							-0.020	
Réal Collobrier (Franchini et al., 1996)												
Resolution (m)	60	120	180	240	360	480					$\Delta/\Delta C$	
K_0 ($m h^{-1}$)	35	70	150	200	450	700					1.58	
K_0/C (h^{-1})	0.58	0.58	0.83	0.83	1.25	1.46					0.002	
Maurets (Saulnier et al., 1997b)												
Resolution (m)	20	40	60	80	100	120					$\Delta/\Delta C$	
K_0 ($m h^{-1}$)	82	184	432	840	822	1402					13.2	
K_0/C (h^{-1})	4.1	4.6	7.2	10.5	8.22	11.68					0.080	
Bore Khola (Brasington and Richards, 1998)												
Resolution (m)	20	40	60	80	100	200	300	400	500		$\Delta/\Delta C$	
K_0 ($m h^{-1}$)	18	24.2	30.4	33.6	46.4	136	150.6	182.4	197.6		0.374	
K_0/C (h^{-1})	0.9	0.61	0.51	0.42	0.46	0.68	0.5	0.46	0.4		-0.001	
Haute-Mentue (Higy and Musy, 2000)												
Resolution (m)	25	30	50	60	75	80	100	110	125	130	150	$\Delta/\Delta C$
T_0 ($m^2 h^{-1}$)	1.13	1.45	1.57	1.91	2.20	3.95	4.19	4.02	4.35	4.87	5.20	0.032
T_0/C ($m h^{-1}$)	0.05	0.05	0.03	0.03	0.03	0.05	0.04	0.04	0.03	0.04	0.03	-0.000
Kamishiiba (Pradhan et al., 2006)												
Resolution (m)	50	150	450	600	1000						$\Delta/\Delta C$	
T_0 ($m^2 h^{-1}$)	6					200						0.204
T_0/C ($m h^{-1}$)	0.12					0.2						0.000

Explicitation of an important scale dependence in TOPMODEL

A. Ducharne

Title Page

Abstract

Introduction

Conclusions

References

Tables

Figures

⏪

⏩

◀

▶

Back

Close

Full Screen / Esc

Printer-friendly Version

Interactive Discussion

Explicitation of an important scale dependence in TOPMODEL

A. Ducharne

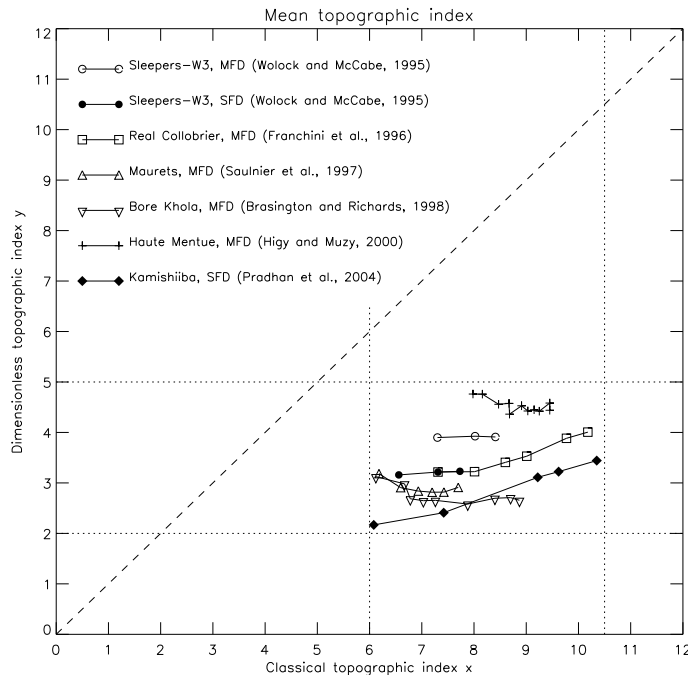


Fig. 1. Comparison of the mean values of the classical and dimensionless TIs, \bar{x} and \bar{y} , for 6 different catchments (distinguished by different symbols) and for different DEM resolutions. The identical symbols along the same line correspond to different resolutions. The values are given in Table 4.

Title Page

Abstract

Introduction

Conclusions

References

Tables

Figures

◀

▶

◀

▶

Back

Close

Full Screen / Esc

Printer-friendly Version

Interactive Discussion



Explicitation of an important scale dependence in TOPMODEL

A. Ducharne

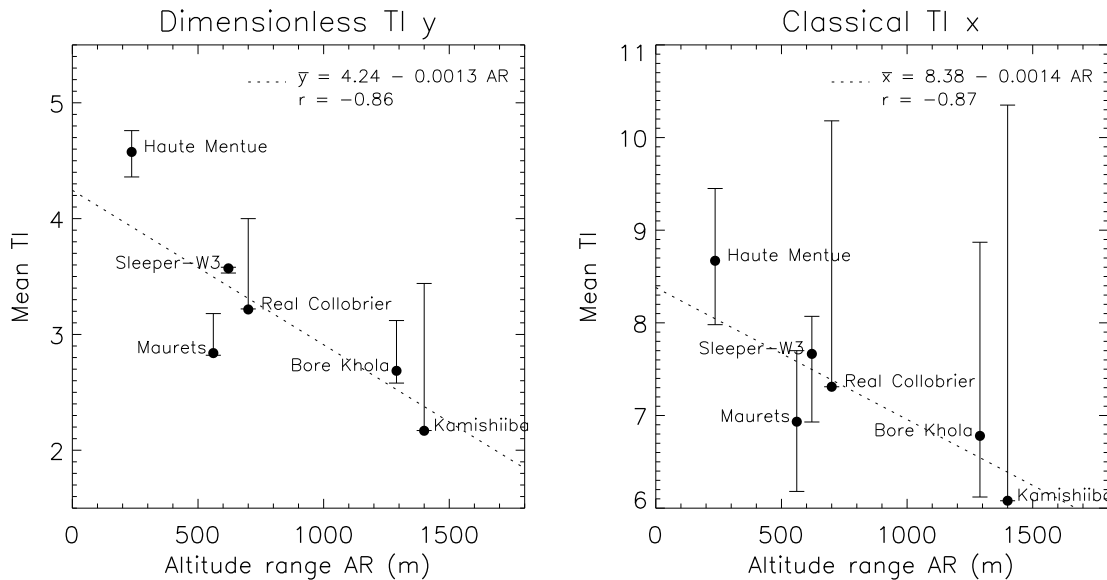


Fig. 2. Relationships between the altitude range (from Table 3) and the mean TIs in the 6 selected catchments: dimensionless TI on the left panel vs. classical TI on the right panel (values from Table 4). The regression lines and correlation coefficients are computed from the mean TIs at the 60-m resolution, used in all the catchments apart from the Kamishiiba catchment, where the 50-m resolution is used instead. For the Sleepers-W3 catchment, we took the average of the mean TIs from the SFD and MFD algorithms. The vertical bars define the range of mean TIs across the different DEM resolutions.

Title Page

Abstract Introduction

Conclusions References

Tables Figures

⏪ ⏩

◀ ▶

Back Close

Full Screen / Esc

Printer-friendly Version

Interactive Discussion